RSC Advances

ROYAL SOCIETY OF CHEMISTRY

www.rsc.org/advances

Journal Name

ARTICLE

Hierarchical Assembly of Enzyme – Inorganic Composite Materials with Extremely High Enzyme Activity

Liwen Liang ,[ab] Xu Fei,*[a] Yue Li,[b] Jing Tian,*[b] Longquan Xu,[a] Xiuying Wang,[a] Yi Wang[b]

Received 00th January 20xx,
Accepted 00th January 20xx

DOI: 10.1039/x0xx00000x

www.rsc.org/

We have synthesized a novel composite material with a hierarchical flower-like structure and extremely high enzyme activity. The spherical, hierarchical flower-like structure with numerous small flowers was formed through self-assembly using papain as organic component and $Cu_3(PO_4)_2 \cdot 3H_2O$ as inorganic component. This hybrid-nanoflower structure was confirmed by Fourier transform infrared spectroscopy, X-ray diffraction. The enzyme activity of papain embedded in the hybrid nanoflowers was further evaluated using BAEE as substrate. Compared with free papain in solution, the hybrid materials exhibited extremely high enzyme activity (~4510%). A study on the relationship of enzyme weight percentage and pattern structure with enzyme activity revealed that enzyme activity was mainly affected by material structure. These results demonstrate that this hierarchical structure can effectively increase enzyme activity.

1. Introduction

Enzyme immobilization is a well-known essential process that improves enzyme stability and storage and that enables the industrial reuse of enzymes for more reaction cycles; thus, enzyme immobilization has extensive applications in sustainable chemical processes.[1] Basically, enzyme immobilization can be divided into the following methods: encapsulation, binding to a support, entrapment, and cross-linking.[2-5] However, some problems still hinder the broad-ranging use of these processes. Most of these methods lead to enhanced stability compared with free enzymes in solution; however, several drawbacks exist, including mass-transfer limitation,[2] activity loss caused by harsh synthesis conditions, and conformational change in enzyme structure.[6] Over the past decade, researchers focus in finding some breakthrough in nano/microsized hybrid materials that can synchronously improve enzyme stability, activity, and lifespan.[7-8] Materials, such as nanoparticles,[9-12] nanotube,[13-14] nanofibers,[15-17] nanocomposite,[18-20] mesoporous material,[21] have already been proposed as substrates in enzymatic immobilization because of their large surface-to-volume ratio.[22]

Recently, Zare et al.[23] have reported an easy method for preparation of enzyme – inorganic hybrid nanoflowers, and this method showed greatly enhanced activities than free enzymes. Subsequently, numerous other researchers have synthesized some hybrid nanoflowers with various enzymes based on the same mechanism.[1,6,24-27] The hierarchical structures of nanomaterials had already been utilized in photocatalysis,[28] solar cells,[29] energy devices,[30] gas sensors,[31] and biomedicine. However, the enzyme – inorganic hybrid nanoflowers have not been fully investigated, especially in the study on the relationship between hierarchical structure and enzyme activity. Therefore, further development is necessary to explore the complete benefits of this type of hybrid materials.

Papain widely exists in papaya roots, stem, and fruits, which belongs to cysteine protease family.[32] Papain is a macro-molecule that consists of 212 amino acid residues; moreover, papain has a 23.5 kDa molecular mass.[33] Considering their abundant raw materials, high thermostability, and wide substrate range, papain has been widely used in biocatalysis, biomedicine, leather, cosmetic, and textile industries,[32-34] and scar therapeutics.[35] A number of methods have ascribed to immobilize papain on different supports.[36-37] However, mass transfer limitation, stability, activity loss, and limited reusability were the main problems for its wider applicability.

In the current study, we synthesized the hierarchical flower-like papain-inorganic hybrid materials using papain, copper chloride aqueous solution, and phosphate buffered saline (PBS) under a certain proportion. The papain-inorganic hybrid materials showed extremely high catalytic activity compared with free papain because of their hierarchical structure. Moreover, the papain-inorganic hybrid materials could be easily isolated from reaction mixture by precipitation. We designed a new method to calculate the amount of enzyme embedded in nanoflowers. Based on our approach, we found that the increase of enzyme activity was mainly affected by the material structure and not by the weight percentage of enzyme in hybrid flower-like materials.

[a] Instrumental Analysis Center, Dalian Polytechnic University, Dalian 116034, P. R. China. E-mail: feixu@dlpu.edu.cn Tel: +86-411-86323691-201 Fax: +86-411-86322038
[b] School of Biological Engineering, Dalian Polytechnic University, Dalian 116034, P. R. China. E-mail: tianjing@dlpu.edu.cn Tel: +86-411-8632448

†Electronic Supplementary Information (ESI) available: [details of any supplementary information available should be included here]. See DOI: 10.1039/x0xx00000x

2.Experimental

2.1Materials

Papain was purchased from Shanghai Yuanye Bio Technology Co., Ltd. Coomassie brilliant blue G-250 was purchased from Tianjin Kemiou Chemical Regent Co., Ltd. $CuCl_2$ was purchased from Shenyang Renagent Industry. Nα-benzoyl-L-arginine ethyl ester (BAEE) was purchase from Aladdin Reagent Co., Ltd. DTT was purchase from Beijing Solarbio Science and Technology Co., Ltd. Other chemicals were analytical reagent grade quality, and used without further purification. All aqueous solutions were prepared using pure water.

2.2 Measurement

The UV-Vis absorption spectra was recorded on a Perkin-Elmer LAMBDA35 (USA). IR spectra was taken on a Spectrum 10 infrared spectrophotometer (Perkin-Elmer, USA). Scanning electron microscopy (SEM) was performed on a JEOL JSM 7800F electron microscope with primary electron energy of 15 kV and transmission electron microscope (TEM) was performed on a JEM2100 with electron energy of 200 kV. The X-ray diffraction (XRD) was measured on a Riguku D/MAX2550 diffractometer with Cu Kα radiation (50 kV, 200 mA, λ =0.154 nm) and a scanning step of 0.02°.

2.3 Synthesis Method

Hybrid flower-like materials were synthesized as follow: 20 μL of aqueous $CuCl_2$ solution (120 mM) was added to 3 mL of PBS (0.1 M, pH=7.4) containing different concentrations of papain. After 3 days incubation at room temperature, the precipitate was collected after centrifugation and rinsing while the supernatant need to be measured by Coomassie Brilliant Blue G250. Then the precipitates were dried by vacuum freeze-drier.

2.4 Determination of Enzyme Activity

The enzyme activity of enzyme-inorgainc hybrid materials was determined by using Nα-benzoyl-L-arginine ethyl ester (BAEE) as substrate. Papain could catalyze the hydrolytic cleavage of the ester linkage in BAEE and produce Nα-benzoyl-L-arginine (BA) which can be detected at 253 nm. The enzyme-inorgainc hybrid nanoflowers (the amount of papain embedded in nanoflowers was equivalent to 0.01 mg papain) were dispersed in 2 mL PBS (0.1 M, pH=7.4) and then mixed with 1 mL activated enzyme solution (30 mM DTT). After incubating for 10 min at 25 °C, the reaction was started by adding 3 mL of 2 mM BAEE and incubated for 5 min. After that, the solution needs to be centrifuged rapidly in order to isolate the enzyme-inorgainc hybrid nanoflowers. The supernatant was detected by UV/Vis absorption and the absorbance was measured at 253 nm. As a comparison, the activity of free papain was determined as the same procedures with 0.01 mg papain as a substitute for the hybrid nanoflowers. One enzyme unit of papain activity will produce a ΔA_{253} of 0.001 per minute with BAEE as substrate at pH 7.4 at 25 °C.

2.5 Determnation of Encapuslation Yield and Enzyme Weight Percentage

2.5.1 Protein Standard Curve

To test the enzyme concentration in the supernatant, we need bovine serum albumin (BSA) to get a protein standard curve. BSA (10 mg) was added to 100 mL NaCl (0.15 mol/mL) to obtain 0.1 mg/ml protein standard solution. Then the above solution was diluted to be 20, 30, 40, 50, 60 and 70 μg/mL with NaCl (0.15 mol/mL). After being added 4 mL Commassie Brilliant Blue G250, the absorptions of solution of different concentrations were detected by UV/Vis absorption spectrophotometer at 595 nm and the protein standard curve of BSA was obtained.

2.5.2 Encapsulation Yield of Enzyme – inorganic Hybrid Flower-like Materials

The encapsulation yield was defined as the ratio of the reduced enzyme amount to the total amount of enzyme employed.[1,6,25] The protein concentration in the supernatant was measured by the Branford protein assay. Commassie Brilliant Blue G250 (4 mL) was added to a tube, which contained supernatant (1 mL, as described in the 2.3). After 5 min, the absorptions of supernatant solution were measured by UV/Vis absorption spectrophotometer at 595 nm. The enzyme concentration in the supernatant was obtained using the standard curve. The calculation of the encapsulation yield was used in the following equation:

$$E = \frac{C_T - C_S}{C_T} \times 100\% \quad (1)$$

where E is the encapsulation yield, C_T is the total amount of enzyme, and C_S is the supernatant enzyme content.

2.5.3 Weight Percentage of Enzyme in Hybrid Flower-like Materials

The weight percentage was defined as the weight ratio of the enzyme, which is actually embedded in nanoflowers to the nanoflower weight. For enzyme content calcinations, the dried hybrid nanoflowers were heated to 700 °C for 3 h at a 10 °C/min heating rate in air. After removal of the organic enzyme in hybrid nanoflowers, the remaining part was inorganic metal salt $Cu_3(PO_4)_2$ (aquamarine blue powder; Fig. S1 (B)). The calculation of weight percentage was used in the following equation:

$$W = \frac{G_N - G_0}{G_N} \times 100\% \quad (2)$$

where W is the weight percentage, G_N is the weight of nanoflowers, and G_0 is the weight of $Cu_3(PO_4)_2 \cdot 3H_2O$.

3. Results and Discussion

3.1 Synthesis and Characterization of Enzyme – inorganic Hybrid Flower-like Materials

To synthesize the enzyme – inorganic hybrid nanoflowers, aqueous $CuCl_2$ solution was added to PBS (0.1 M, pH 7.4) that contained different papain concentrations for 3 days at room temperature. After rinsing and freeze drying, we obtained hybrid nanoflowers (Fig. S1 (A)), and the formation progress was illustrated in Fig. 1. The general morphologies of the enzyme – inorganic hybrid nanoflowers were determined by scanning electron microscopy (SEM) and transmission electron microscopy (TEM). All these figures demonstrate that the

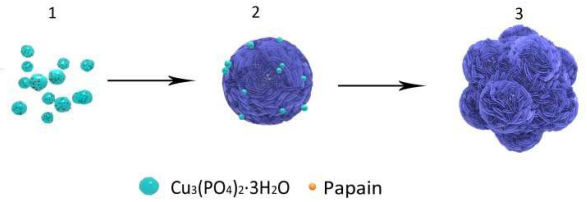

Fig. 1 Proposed growth mechanism of nanoflowers.

hybrid nanoflowers had uniform appearance with good monodispersity (Figs. S2A – S2D in Supporting Information). As organic molecules complexing agent, enzyme has strong complexation with metal ions; thus, nucleation, growth, and assembly depend on the enzyme concentration. We can observe that the increase in papain concentration (i.e., 0.25, 0.5, 1.0, and 2.0 mg/mL) induced a significant morphology change (Figs. 2A – 2D). The TEM image of a single nanoflower (formed with 0.25 mg/mL papain) was shown in Fig. 3 In addition, the high-resolution SEM images showed that the petals of hybrid nanoflowers became more compact and intense, as shown in Figs. S3A – S3D (see Supporting Information). By contrast, with increased papain concentration, the average diameters of these nanoflowers decreased approximately from 20 μm to 9 μm. These results reveal that papain concentration can influence the number of nucleation sites and thus affect the size and structures of hybrid nanoflowers. Notably, no nanoflowers formed with decreased papain concentration to 0.125 mg/mL; however, the process only formed irregular papain-Cu^{2+} crystals petals. (Fig. S4 (B) in Supporting Information)

To study the formation mechanism of hierarchical flower-like structure, different incubation times (i.e., 0.5, 3, 6, 12, 24, and 48 h) were applied while the papain concentration (0.25 mg/mL) was kept constant. SEM images revealed the

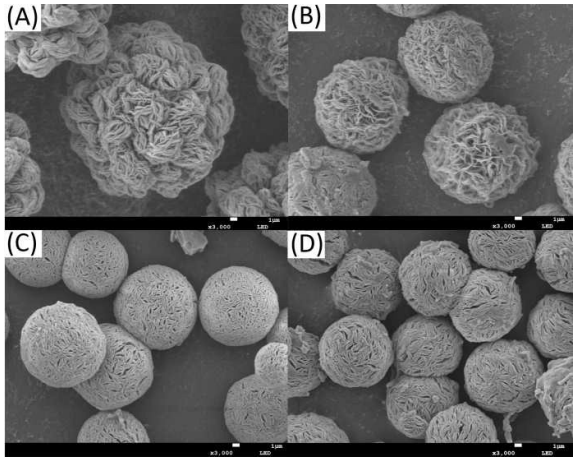

Fig. 2 SEM images of nanoflowers with different concentration of papain:(A) 0.25 mg/mL; (B) 0.5 mg/mL; (C) 1.0 mg/mL; (D) 2.0 mg/mL.

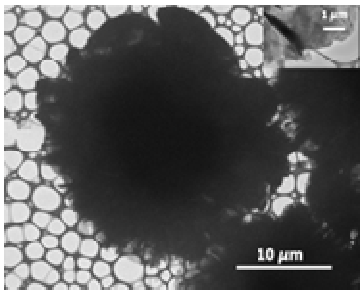

Fig. 3 TEM image of nanoflowers formed with 0.25 mg/mL papain.

structures obtained at each time point. Result shown in Fig. S5 (see Supporting Information) suggested a progressive process of nanoflower assembly. There is no obvious change for the enzyme molecule at 0.5 h (Fig. S5 (A)). Some papain-$Cu_3(PO_4)_2 \cdot 3H_2O$ crystals were formed at 3 h initially (Fig. S5 (B)). After 6 h of incubation, the papain complexes with Cu^{2+} provided a location for nucleation of the primary crystals; moreover, these complexes further agglomerated to form the primary petals (Fig. S5 (C)). The size of the complexes became larger at 12 h (Fig. S5 (D)). With increased incubation time (24 and 48 h; Fig. S5 (E) and S5 (F) in Supporting Information), the papain-Cu^{2+} crystal scaffold aggregated more petals that bound to the nanoflower surface and finally produce a hierarchical flower-shape structure. This result was in accordance with our proposed growth mechanism of nanoflowers in Fig. 1.

The structure of hybrid nanoflowers formed with different papain concentrations was confirmed by FT-IR. As an example, Fig. 4A (b) reveals strong characteristic absorption (spectrum a) at 1042 (asymmetric stretching), 988 (symmetric stretching), and 623 cm^{-1} (bending), all of which may be attributed to P–O vibrations. These signals indicated the presence of phosphate groups. In spectrum g, typical papain absorption peaks occurred at 1655 and 1538 cm^{-1} for –CONH, 2800 cm^{-1} to 3000 cm^{-1} for $-CH_2$ and $-CH_3$, and around 3300 cm^{-1} for –OH. Comparison of spectra c, d, e, and f indicated that the characteristic absorption peaks of papain and $Cu_3(PO_4)_2 \cdot 3H_2O$ were maintained in IR spectra. With the increase of papain concentration, the characteristic papain absorption in the nanoflowers increased gradually until 1.0 mg/mL (curve d). Over this concentration, excessive enzymes were not able to participate in the hybrid composite materials. Thus, papain concentration was a key factor in the synthesis of organic–inorganic nanoflowers.

The XRD patterns in Fig. 4B revealed that the crystallographic structures of the nanoflowers was $Cu_3(PO_4)_2 \cdot 3H_2O$. All diffraction peaks in Figs. 4B (a) and 4B (b) could be indexed to JCPDS Card No. 22-0548 [Fig. 4B (c)]. Therefore, the hybrid nanoflowers were well crystallized and featured high crystallinity after papain incorporation.

The methods of determining papain encapsulation yield and weight percentage in hybrid nanoflowers were the same as the above mentioned description. The results of encapsulation yield and weight percentage of papain in hybrid nanoflowers,

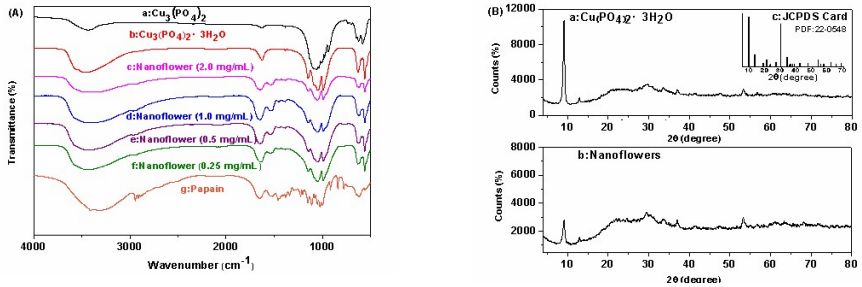

Fig.4 (A) FT-IR spectra of the hybrid nanoflowers formed with different concentrations (a) $Cu_3(PO_4)_2$; (b) $Cu_3(PO_4)_2 \cdot 3H_2O$; (c) 2.0 mg/mL; (d) 1.0 mg/mL; (e) 0.5 mg/mL; (f) 0.25 mg/mL; (g) Free papain. (B) XRD patterns of (a) $Cu_3(PO_4)_2 \cdot 3H_2O$, (b) hybrid nanoflowers formed with 0.25 mg/mL papain and (c) JCPDS Card No. 22-0548.

which were formed with $CuCl_2$ from 0.25 mg/mL to 2.0 mg/mL, were shown in Table 1 and 2. The encapsulation yield of papain was found to decrease from 81.73% to 68.48% with the increased papain concentration. After calcination at 700 ^{o}C, hybrid materials were transformed into phosphoric acid copper (Fig. S6 in Supporting Information). Therefore, we can calculate the weight of $Cu_3(PO_4)_2 \cdot 3H_2O$ in hybrid nanoflowers by comparing $Cu_3(PO_4)_2$ and obtain the weight percentage of papain in nanoflowers finally. The weight percentage of papain in hybrid nanoflowers were 3.56%, 4.74%, 11.04% and 39.15% at different papain concentration (from 0.25 mg/mL to 2.0 mg/mL).

3.2 Enzyme Activity and Kinetics of Enzyme – inorganic Hybrid Flower-like Materials

The enzyme activity of papain in the hybrid flower-like materials formed using 0.25, 0.5, 1.0, and 2.0 mg/mL papain in solution were determined to be approximately 8253, 3362, 1329, and 78 U/mg, respectively, compared with free papain where its corresponding activity was approximately 183 U/mg. The change in enzyme activity between these concentrations may be due to the difference in nanoflower structure (Figs. S2 A-D in Supporting Information). For hierarchical structure formation, the enzyme (as an organic complexing agent) directly affected the number of nucleation sites. Therefore, enzyme concentration in the reaction system affected the pattern structure, including size and density. The main factor in the enzyme – inorganic hybrid flower-like materials to increase enzyme activity is the enzyme can be well dispersed in the large surface area of nanoflowers compared with free enzyme, and this enzyme can fully make contact with the substrate.

The increase in catalytic activity was due to the high surface area of nanoflowers, which resulted in high substrate accessibility to the papain active sites. However, when the papain concentration was extremely high such that excessive impact nanopetals were formed (Fig. S2 (D) in Supporting Information), nanoflower catalytic activity was affected. With increased papain concentration from 0.25 mg/mL to 2.0 mg/mL, enzyme activity dramatically dropped from approximately 8253 U/mg to approximately 78 U/mg. We assumed that the reason may be transfer limitation. We assumed that the reason may be transfer limitation due to the different density of the petals.

Based on the results of our experiment, the hybrid nanoflowers synthesized with 0.25 mg/mL papain was chosen for kinetics study. The catalytic activity of the hybrid nanoflowers and free papain were evaluated using BAEE as the substrate. The initial concentration of BAEE was set to be 2 mM. Upon the addition of free papain, absorbance at 253 nm increased slowly over time. In hybrid nanoflowers system (the concentration of papain put in was 0.003 mg/mL), absorption enhanced significantly, indicating the high catalytic efficiency of the nanoflowers. The pseudo-first-order kinetics with BAEE could be applied to our experimental system. As shown in Fig. 5, the approximately linear shape of the plot of -ln I_{sub} (i.e., I_{sub}

Table 1. The encapsulation yield of papain in the nanoflowers

Enzyme concentration (mg/mL)	Actual concentration (mg/mL)	The supernatant concentration (mg/mL)	Encapsulation yield (%)	The average value of encapsulation yield (%)	Enzymatic activity (U/mg)
0.25	0.2517	0.0446	82.30		
0.25	0.2521	0.0451	82.11	81.73±0.83	8254±285
0.25	0.2502	0.0481	80.77		
0.50	0.4999	0.0880	82.46		
0.50	0.5031	0.0957	80.97	81.10±1.30	3363±245
0.50	0.5006	0.1008	79.86		
1.00	0.9989	0.2193	78.15		
1.00	0.9978	0.2073	79.22	77.00±0.72	1329±44
1.00	1.0033	0.2223	77.84		
2.00	2.0022	0.6029	69.89		
2.00	2.0056	0.5992	70.13	69.75±0.46	78±4
2.00	2.0011	0.6156	69.24		

Table 2. The weight percentage of papain in the nanoflowers

Enzyme concentration (mg/mL)	Nanoflowers (g)	$Cu_3(PO_4)_2$ (g)	$Cu_3(PO_4)_2 \cdot 3H_2O$ (g)	Weight percentage of enzyme (%)	The average value of weight percentage (%)
0.25	0.2211	0.1871	0.2136	3.49	
0.25	0.1986	0.1673	0.1910	3.96	3.57±0.36
0.25	0.2510	0.2129	0.2431	3.25	
0.5	0.2177	0.1830	0.2090	4.01	
0.5	0.2072	0.1715	0.1958	5.49	4.74±0.74
0.5	0.2228	0.1859	0.2123	4.72	
1.0	0.2065	0.1603	0.1830	11.35	
1.0	0.2250	0.1769	0.2020	11.38	11.03±0.58
1.0	0.2184	0.1733	0.1979	10.36	
2.0	0.1225	0.0752	0.0859	42.66	
2.0	0.2176	0.1396	0.1594	36.51	39.15±3.17
2.0	0.1290	0.0817	0.0933	38.28	

was the value obtained by substracting real-time absorbance from the saturated one) vs. time supports the pseudo-first-order assumption. Based on such linear relationship, the average values of the reaction rate constant (k) were calculated to be 6.44×10^{-3} s^{-1} and 1.79×10^{-3} s^{-1} when hybrid nanoflowers and free papain were used, respectively.

To test the reusability of the hybrid nanoflowers, the nanoflowers formed using 0.25 mg/mL papain were used for their high enzyme activity. Each time, after reacting with BAEE, the hybrid nanoflowers were centrifuged and washed three times with pure water. Subsequently, the precipitate was subjected to the next catalytic cycle. Supernatant absorption at 253 nm for the first measurement was set as 100%. As shown in Figure 6, although enzyme activity was reduced to 28.90% after the fifth reaction cycle, activity was still much higher than that of free papain (Table 1 in Supporting Information).

In order to find out the reason why the enzyme activity decrease, we collected the nanoflowers (0.25 mg/mL) after reacting only with BAEE and washed three times before being observed by scanning electron microscopy. From the Fig. S8, it was found that the petals density of the nanoflowers had decreased. We assumed that the reduction of hierarchical structure led to the decreasing of enzyme activity.

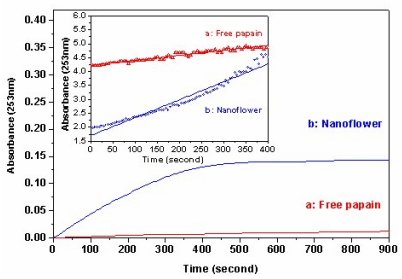

Fig. 5 Catalytic kinetics and reaction rate (insert part) of the esterlysis of BAEE by free papain (a) and hybrid nanoflowers (b).

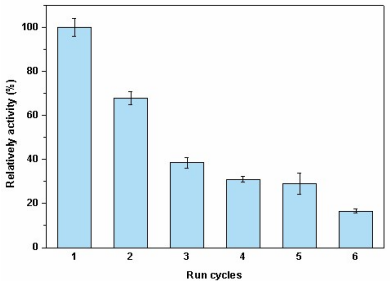

Fig. 6 Effect of recycling on the activity of hybrid nanoflowers (0.25 mg/mL).

Conclusion

We synthesized a kind of composite material with a hierarchical flower-like structure and extremely high enzyme activity. We then applied a new method to calculate the amount of papain that was actually embedded in nanoflowers to increase the accuracy of enzyme-activity calculation. And we found the main factor affecting the catalytic activity of the material was material structure and not actual enzyme weight percentage. Therefore, papain concentration can affect nanoflower structure and subsequently affect enzyme activity. These findings have great significance in the synthesis of these hybrid materials.

Acknowledgements

This work was supported by National Natural Science Foundation of China (No.21204007), Excellent talents support program of colleges and universities of Liaoning province (LJQ2014054), Natural Science Foundation of Liaoning Province of China (2013020167), Open Project of State Key Laboratory for Supramolecular Structure and Materials (SKLSSM201425)

References

1 L. B.Wang, Y. C. Wang, R. He, A. Zhuang, X. P. Wang, J. Zeng and J. G. Hou, *J. Am. Chem. Soc.*, 2013, **135**, 1272-1275.
2 E. T. Hwang and M. B. Gu, *Eng. Life Sci.*, 2013, **13**, 49-61.
3 S. Hrapovic, Y. L. Liu, K. B. Male and J. H. T. Luong, *Analy. chem*., 2004, **76**, 1083-1088.
4 D. Ma, M. Li and A. J. Patil, *Adv. Mater.*, 2004, **16**, 1838-1841.
5 C. Z. Dinu, I. V. Borkar, S. S. Bael, A. S. Campbell, R. S. Kane and J. S. Dordick, *J. Mol. Catal. B-Enzym.*, 2012, **75**, 20-26.
6 Z. Lin, Y. Xiao, Y. Yin, W. Hu and H. Yang, *ACS Appl. Mater. Inter.*, 2014, **6**, 10775-10782.
7 C. X. Lei, S. Q. Hu, N. Gao, G. L. Shen and R. Q. Yu, *Bioelectrochemistry.* , 2004, **65**, 33-39.
8 J. Kim, H. Jia and P. Wang, *Biotechnolo. Adv.*, 2006, **24**, 296-308.
9 S. Sayin, E. Yilmaz and M. Yilmaz, Org. *Biomol. Chem*., 2011, **9**, 4021-4024.
10 J. Hu, G. Zhang and S. Liu. *Chem. Soc. Rev.*, 2012, **41**, 5933-5949.
11 B. Saha, J. Saikia and G. Das, *Analyst.*, 2015, **140**, 532-542.
12 L. R. Nemzer, A. Schwartz and A. J. Epstein, *Macromolecules.*, 2010, **43**, 4324-4330.
13 M. E. G. Lyons and G. P. Keeley, *Chem. Commun.*, 2008, 2529-2531.
14 P. Kohli and C. R. Martin, *Curr. Pharm. Biotechno.*, 2005, **6**, 35-47.
15 E. Shoba, R. Lakra, M. S. Kiran and P. S. Korrapati, *RCS Adv.* 2014, **4**, 60209-60215.
16 S. M. Lee, L. H. Jin, J. H. Kim, S. O. Han, H. B. Na, T. Hyeon, Y. M. Koo, J. Kim and J. H. Lee, *Bioproc. Biosyst. Eng.*, 2010, **33**, 141-147.
17 T. E. Herricks, S. H. Kim, J. Kim, D. Li, J .H. Kwak, J. W. Grate, S. H. Kim and Y. N. Xia, *J. Materi. Chem.*, 2005, **15**, 3241-3245.
18 U. Baig, M. A. Gondal, M. F. Alam, A. A. Laskar, M. Alam and H. Younus, *New J. Chem.* 2015, **39**, 6975-6986.
19 M. L. Verma, C. J. Barrow and M. Puri, *Appl. Microbiol. Biot.*, 2013, **97**, 23-39.
20 M. Kalantari, M. Kazemeini, F. Tanamdeh and A. Arpanaei, *J.Mater.Chem.*, 2012, **22**, 8385-8393.
21 Z. Zhou and M. Hartmann, *Chem Soc. Rev.*, 2013, **42**, 3894-3912.
22 S. A. Ansari and Q. Husain, *Biotechnol. Adv.*, 2012, **30**, 512-523.
23 J. Ge, J. Lei and R. N. Zare, Nat. *Nanotechnol.*, 2012, **7**, 428-432.
24 J.Sun, J Ge, W. Liu, M. Lan, H. Zhang, P. Wang and Z. Niu, *Nanoscale.*, 2014, **6**, 255-262.
25 Z. Lin, Y. Xiao, L. Wang, Y. Yin, J. Zheng, H. Yang and G. Chen, *RSC Adv.*, 2014, **4**, 13888-13891.
26 Z. Wu, X. Li, F. Li, H. Yue, C. He, F. Xie and Z. Wang, *RSC Adv.*, 2014, **4**, 33998-34002.
27 I. Ocsoy, E. Dogru and S. Usta, *Enzyme Microb. Tech*., 2015, **75**, 25-29.
28 C. Xu, L. Cao, G. S. Wei, W. Liu, H. Liu, Y. Yu and X. Qu, J. Hazard. *Mater.*, 2010, **176**, 807-813.
29 C. Xu, P. Shin, L. Cao and D. Gao, *J. Phys. Chem. C*., 2010, **114**, 125-129.
30 X. Dong, G. Sui, A. Guo, H. Du and J. Liu, *Chem. Eng. J.* , 2015, **277**, 159-167.
31 X. Xue, Z. Chen, C. Ma, L. Xing, Y. Chen, Y. Wang and T. Wang, *J. Phys. Chem. C.*, 2010, **114**, 3968-3972.
32 N. Zou and J. Plank, *J. Phys. Chem. Solids.*, 2012, **73**, 1127-1130.
33 A. Manosroi, C. Chankhampan, W. Manosroi and J. Manosroi, Eur. *J. Pharm. Sci.*, 2013, **48**, 474-483.
34 C. R. Llerena-Suster, C. José, S. E. Collins, L. E. Briand and S. R. Morcelle, *Process. Biochem.*, 2014, **47**, 47-56.
35 J. K. Lai, T. H. Chuang, J. S. Jan and S. S. S. Wang, *Colloid. Surfaces. B.* , 2010, **80**, 51-58.
36 L. Han, W. Wang, L. L. Chen, X. C. Li, B. Yi and L. Deng, *Enzyme Microb. Technol.*, 2004, **35**, 15-21.
37 S. S. Khapard and R. S. Singhal, *Bioresource Technol.*, 2001, **78**, 1-4.

Graphical Abstract

We have synthesized a kind of composite material with a hierarchical flower-like structure and extremely high enzyme activity. We then applied a new method to calculate enzyme-activity of composite material accurately. And we found that the main factor affecting the catalytic activity of the material was material structure and not actual enzyme weight percentage.